

MARS-KS Analysis of Low Pressure Low Flow Critical Heat Flux Based on Annulus and Round-Tube Experimental Data

Nhan Hien Hoang^{a*}, Seong-Su Jeon^a, Jehhee Lee^a, Ju-Yeop Park^b

^aFNC Technology, Co., Ltd., 593 Daedeok-daero, #1004-1, Yuseong-gu, Daejeon, 34112, Korea

^bKorea Institute of Nuclear Safety, 62 Gwahak-ro, Yuseong-gu, Daejeon 334142, Korea

*Corresponding author: hnhien@fnctech.com

***Keywords** : critical heat flux, low pressure, low flow, SMR, MARS-KS

1. Introduction

Critical Heat Flux (CHF) under the Low Pressure Low Flow (LPLF) condition has been intensively investigated in relation to normal and/or accident conditions of light water reactors, research reactors and now even for Small Modular Reactors (SMRs) these days [1,2]. According to Yang et al. [2], most CHF data collected so far mostly cover High Pressure and High Flow (HPHF) range such as 10.0~17.5 MPa for pressure and 1695~4746 kg/(m²·s) for mass flux. Therefore, below 10.0MPa in pressure and 1695 kg/m²s in mass flux may be considered as LPLF condition in the present study [3].

The increasing attention to LPLF CHF for SMRs is due to the fact that thermal-hydraulic condition of SMRs may experience LPLF while the level of water being above the reactor core under LOCA and as a result, avoiding CHF is accepted as a new acceptance criterion for SMRs.[4]

However, studying CHF under LPLF condition is quite challenging because flow instabilities which are more engaging under LPLF condition due to large specific volume ratio between liquid and vapor under low pressure and dominant buoyancy under low flow may impact a steady state LPLF CHF and a result, a premature CHF could happen under LPLF condition. This is also the reason why there are not many CHF test data available in LPLF range because flow instabilities may damage experimental facilities with unexpected manner.

In view of growing importance of LPLF CHF, in the present study, we assess MARS-KS code's CHF models such as AECL CHF Lookup Table and Knoebel Annuli CHF correlation [5] against annulus [6] and round-tube [1] experiments which both were conducted under LPLF conditions.

2. Low Pressure Low Flow CHF Analysis

In this section, MARS-KS code analysis results were presented for two LPLF CHF experimental dataset typical of the round tube and annular geometries [1,6]. The simple test geometries were selected to highlight findings while minimizing unknown effects. After that, such effect as non-uniform heating, indirect heating and surface properties were additionally investigated for identifying their impacts on LPLF CHF.

2.1 LPLF CHF Experimental Data

The analysis in this study is mainly based on the first CHF dataset for flow boiling of water in a short annular channel of 326 mm length uniformly heated from inner side by a zircaloy tube of 9.5 mm outer diameter [6]. The dataset has 70 points covering mass flux of 111.4–298.7 kg/m²s, outlet pressure of 0.12–0.4 MPa, inlet subcooling of 115–293 kJ/kg, and the heating power of 3–75 kW.

The second dataset of 240 CHF data points of water in vertical round Inconel-625 tubes [1] with the heated length of 0.3–1.77 m, pressure of 0.106–0.951 MPa, mass flux of 20–277 kg/m²s, and inlet subcooling of 50–654 kJ/kg was selected to provide a comparison with the first one.

2.2 MARS-KS Code Analysis Models

Simple MARS-KS code analysis models simulate fluid channels by a pipe component of different sizes. The inlet pressure, inlet temperature, and mass flow rate were set to constants as the experiment. The outlet conditions were allowed to change during heating. For direct heating, the heating power was applied directly to the heat structure simulating the heater rod. For indirect heating, the heat flux was applied to the inner side of the rod. Both the heating power and heat flux were gradually increased to the target value within 5000 seconds. If a high surface temperature excursion occurs within this period and the calculation was failed to continue, then the last rod heat flux is taken as the actual CHF (q''_w) besides the CHF predicted by CHF models/correlations ($q''_{CHF,c}$). In addition, the effect of surface condition changes was investigated by modifying the thermal conductivity of $\pm 30\%$.

The critical heat flux was predicted by ACEL CHF Look Up Table (LUT) and the KNOEBEL Annuli CHF correlation [5], and it was compared with the experimental values. The Katto liquid sublayer dryout (LSD) model [7] and the pool-boiling CHF limit [8] given by Eqns. (1-2) were additionally assessed against the annular CHF data for modeling considerations.

$$q''_{Katto} = \delta \rho_L h_{fg} / \tau \quad (1)$$

$$q''_{PB} = 0.13 h_{fg} (\rho_g^2 \sigma g \Delta \rho)^{1/4} \quad (2)$$

where h_{fg} is the latent heat, g is the gravity, δ is the liquid layer thickness, σ is the surface tension, τ is the passage time, and $\Delta\rho$ is the density difference.

2.3 Analysis Results

A sensitivity analysis was conducted first for the length of calculation cell. The test section was divided into 10, 20, 30, 40, and 50 nodes. The CHF calculated using the mesh of 20 nodes showed the smallest difference from the experimental value. Therefore, this mesh was selected for further calculations.

Figure 1 shows the variation of the rod surface temperature with power increase at upper nodes. The surface temperature quickly increased at the initial stage and then slightly changed (even the power continuously increased) until a sharp rise occurred. The temperature rise was observed at the top node first then to the lower nodes. The heat flux value at which the temperature rise occurs was determined as the predicted CHF value.

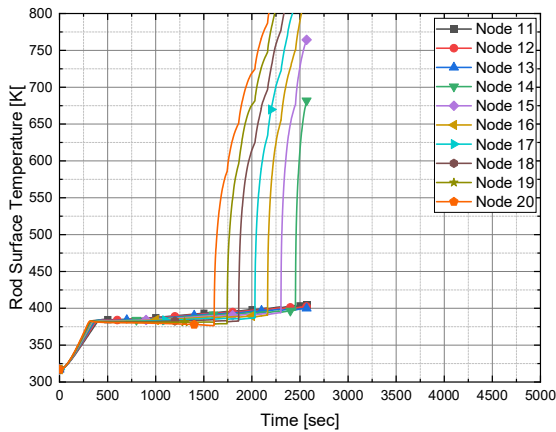


Fig. 1. Surface temperature variation

Observation of qualities in Fig. 2 shows a linear increase of thermodynamic quality (or liquid temperature) and a complex variation of flow quality with power increase. Flow at the CHF was in the annular pattern, and flow instability due to pressure drop was indicated.

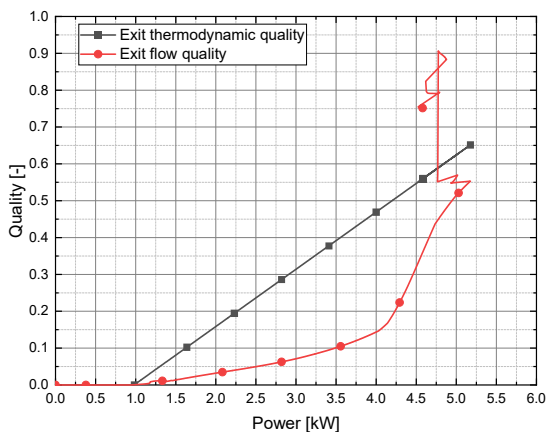


Fig. 2. Variation of qualities with power increase

Figure 3 shows the ratio of CHF predicted by MARS-KS code (2006 CHF LUT) to the experimental CHF values. The CHF LUT tends to overpredict the Kim et al. (2000) CHF data, about 48%, especially in the region of low heat flux where the LPLF condition is prevailing. Meanwhile, the opposite trend was observed with Hass (2012) CHF data. MARS-KS calculation only showed temperature rise for 32 of 57 cases of the Hass data. This means the power was not reach the level at which CHF occurs for the remaining cases. Comparison with the flooding limit showed the occurrence of flooding CHF at heat fluxes less than 400 kW/m².

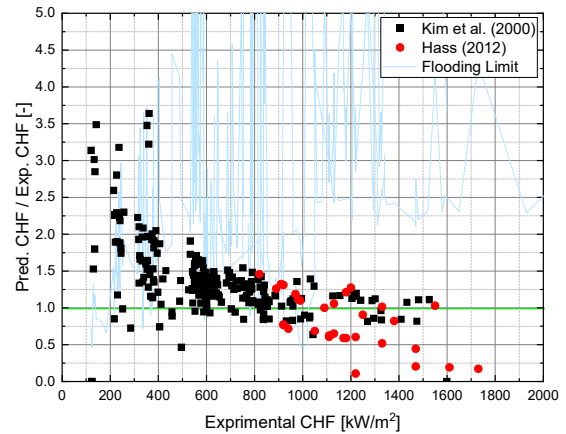


Fig. 3. CHF ratio varying with wall heat flux

As shown in Figs. 4-5, the overprediction of CHF mainly occurred at pressure lower than 500 kPa and flow rate lower than 120 kg/s. These calculation results showed a limited applicability of the 2006 CHF LUT to the LPLF CHF data. First, the ranges of pressure and flow rate of the CHF LUT were not fine enough over the LPLF region and some tabular points are unreal. Second, flow instability (e.g., Ledinegg instability) is dominant in the LPLF region. For this region, a lower limit should be defined. Finally, the MARS-KS code was mainly developed for high pressure and high flow conditions of nuclear reactors. Therefore, the applicability of its closure models to the LPLF region is still questionable.

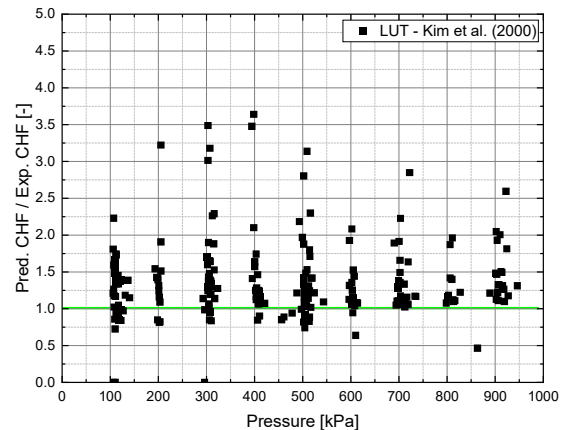


Fig. 4. CHF ratio varying with system pressure

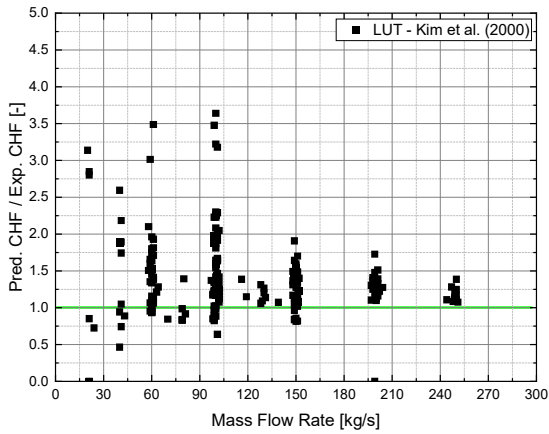


Fig. 5. CHF ratio varying with mass flow rate

Figure 6 showed the effect of heating method on the CHF for Kim et al (2000) data. The direct and indirect heating just showed a significant effect at the lower heat fluxes. At the high heat fluxes, the radial heat conduction dominates the axial heat condition and hence the effect of heating method was eliminated.

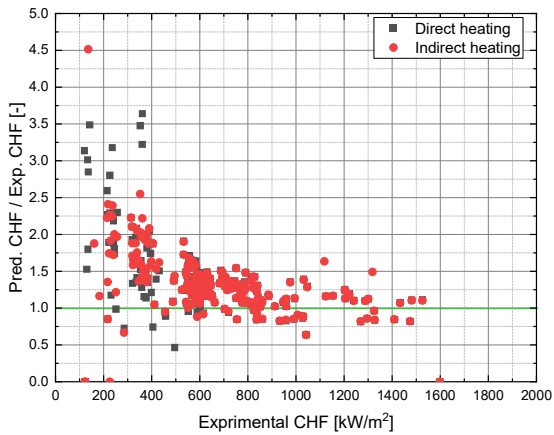


Fig. 6. Comparison of direct and indirect heating methods

The effect of nonuniform heating considered based on Kim et al. (2000) data by apply a cosine power profile to the heat structure simulating the heater rod, and it was presented in Figs. 7-8. Unlike the uniform heating case, the surface temperature rise occurred at an upper node (e.g., node 18 in case 1 of Kim et al. data) near the power peak not the node at the top. The temperature rise happened much earlier than the cases of uniform heating. The predicted CHF values for nonuniform heating were higher than those for uniform heating and higher than the experimental values. The difference was caused by the difference in local flow condition when applying a nonuniform power profile. Especially, since the heated length of consideration was short, 0.3–1.77 m, the nonuniform heating became significant due to axial high heat flux gradient.

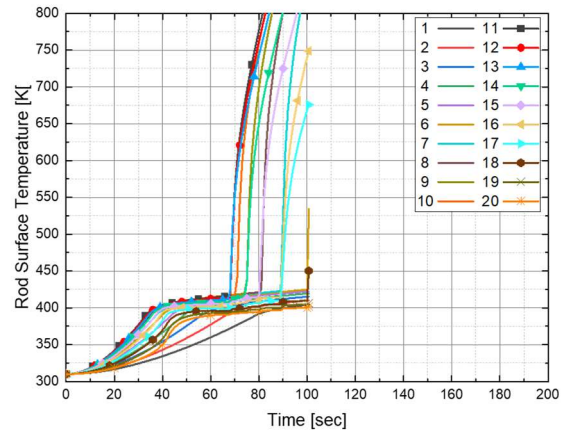


Fig. 7. Surface temperature variation: Nonuniform heating

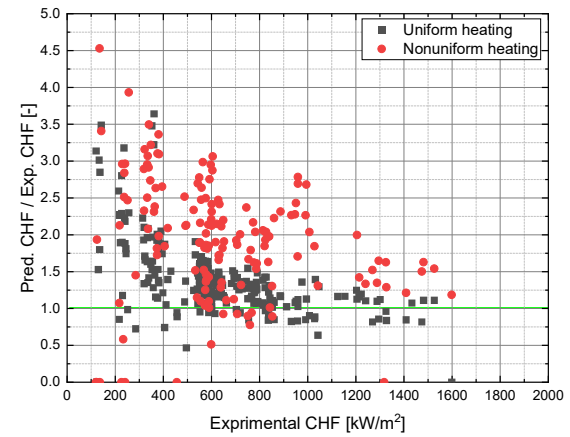


Fig. 8. Nonuniform heating effect on CHF

The KNOEBEL Annuli CHF correlation was assessed against Hass (2012) CHF data for annulus flow channel. Unexpectedly, no MARS-KS calculations showed a surface temperature rise or CHF occurrence. Thus, it is recommended to do not use this correlation.

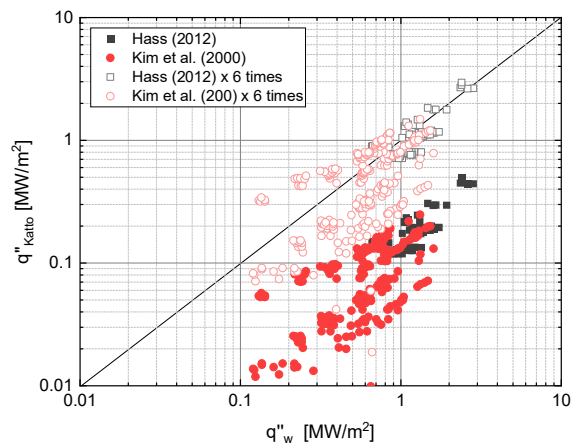


Fig. 9. Predicted results of Katto (1990) model

Finally, an interesting finding was noted based on the assessment of Katto SLD model against the experimental

CHF data (see Fig. 9). Although the Katto model was about six times underpredicted, the predicted CHF values seem to have the same trend of that of the experimental CHF data.

Since the ratio of vapor density to liquid density is very small at a very low pressure, vapor bubble will be large and liquid sublayer may be very thin. Meanwhile, the passage time of vapor bubble was estimated by dividing bubble length by bubble velocity, and the bubble velocity was determined using the universal turbulent velocity profile. Therefore, it is guessed that the calculation of bubble velocity largely contributed to the underprediction of the Katto model. A better prediction can be obtained using the Katto model if improving the determination of bubble parameters.

When using a theoretical model in the frame of a system/subchannel thermal-hydraulic analysis code (e.g., MARS-KS), it also needs to check the compatibility of this model with other closure modes of the code, such as the application range of the models.

3. Conclusions

The low pressure low flow (LPLF) critical heat flux (CHF) was evaluated through the MARS-KS code analysis of annulus and round-tube CHF experimental data. The 2006 CHF lookup table and the KNOEBEL Annuli CHF correlation implemented in MARS-KS code significantly overpredicted the CHF data, especially in the region of very low mass flux and very pressure. Therefore, the application of the CHF lookup table and CHF correlations to the LPFL conditions as in SMRs should be critical considered.

The application of MARS-KS analysis code to prediction of LPLF CHF could be limited since the MARS-KS closure models were mainly developed for a high-pressure high-flow condition.

The effect of flow instabilities under the LFLP and low subcooling condition was identifiable. However, it may not be easy to estimate precisely its impact on the LPLF CHF. Therefore, a lower limit such as flooding limit should be considered at the same time.

The effect of nonuniform heating was significant, especially for short heating length, due to a large axial heat flux gradient.

Finally, the Katto's CHF model that based on the sublayer dryout hypothesis could be a good starting point for modeling of LPLF CHF.

Acknowledgment

We acknowledge that this research has been conducted with a support from the national nuclear safety research titled "Study on Validation of Consolidated Safety Analysis Platform for Applications of Enhanced Safety Criteria and New Nuclear Fuels (Contract No. 2106002)"

funded by Nuclear Safety and Security Commission of KOREA.

REFERENCES

- [1] H. C. Kim, W. P. Baek, S. H. Chang, Critical Heat Flux of Water in Vertical Round Tubes at Low Pressure and Low Flow Conditions, *Nuc. Eng. Des.* Vol. 199, p.49-73, 2000.
- [2] B.W. Yang, B. Han, A. Liu, Low Pressure Low Flow Rod Bundle CHF and Its Challenges in SMR, NURETH-20, Washington D.C., Aug 20-25, 2023.
- [3] J. Y. Park, Opinion Paper SMR CHF Issues, Project Review Meeting Presentation, Korea Institute of Nuclear Safety, January 2025.
- [4] US NRC, Safety Evaluation Report on NuScale Design Certificate Review, Chap. 15.0.2 & 15.6.5, 20, August 2000.
- [5] MARS Code Manual, Volume I: Code Structure, System Models, and Solution Method.
- [6] C. Hass, Critical Heat Flux for Flow Boiling of Water at Low Pressure on Smooth and Micro-Structured Zircaloy Tube Surfaces, *KIT Scientific Reports* 7627, 2012.
- [7] Y. Katto, A Physical Approach to Critical Heat Flux of Subcooled Flow Boiling in Round Tubes, Vol. 33, p. 611-620, 1990.
- [8] K. Mishima, H. Nishihara, Effect of Channel Geometry on Critical Heat Flux for Low Pressure Water, *Int. J. Heat Mass Transfer*, Vol. 30, p.1169-1182, 1987.